Multiphase contrast-enhanced computed tomography imaging features of salivary duct carcinoma: differentiation from other salivary gland malignancies

Wen-li Wu, MM,[a] Cheng-long Wang, MM,[b] Dan Li, MD,[c] Jin Luo, MM,[d] Jun-yong Ye, DE,[d] and Sheng-sheng Xu, MD[a]

Objective. The aim of this study was to investigate the imaging features of salivary duct carcinoma (SDC) with multiphase contrast-enhanced computed tomography (CECT) and to compare them with those of mucoepidermoid carcinoma (MEC), adenoid cystic carcinoma (ACC), and acinic cell carcinoma.

Study Design. A total of 63 patients with histologically diagnosed salivary gland malignancies underwent preoperative multiphase CECT. Clinical information, location, size, mass pattern, enhancement pattern, borders, invasion of adjacent tissues, and lymph node metastasis were evaluated. Computed tomography (CT) number attenuation patterns were calculated.

Results. SDCs were significantly more common in males and in the parotid gland ($P \leq .018$). They were more likely to invade into adjacent tissues and metastasize to lymph nodes ($P \leq .032$). Six SDCs (66.7%) had comedonecrosis, as detected on histopathologic examination, and 3 lesions presented cribriform necrosis on CECT. CT numbers during delayed-phase scanning were significantly higher in SDC than in ACC ($P = .031$). Significant differences were discovered between MEC and ACC for CT numbers during arterial-phase scanning ($P = .047$) and in the ratio of CT numbers ($P = .018$).

Conclusions. SDC exhibits some specific CT features, and multiphase CECT imaging is useful in the differential diagnosis of salivary gland malignancies. (Oral Surg Oral Med Oral Pathol Oral Radiol 2019;128:543−551)

Malignant salivary gland tumors are rare, but there are diverse histopathologic types.[1,2] Among them, salivary duct carcinoma (SDC) is estimated to represent approximately 1% to 3% of all salivary malignancies, and SDC is the most frequent type of high-grade salivary gland tumors.[3−6] SDC is characterized by aggressive behavior, early nodal and distant metastases, and a high rate of local recurrence. Complete surgical resection of the tumor and neck dissection, followed by adjuvant locoregional radiotherapy, are generally recommended for patients with SDC. Therefore, differentiating the histologic types among malignant lesions is necessary before surgery. Some studies have investigated the imaging features of SDC.[7−9] However, descriptions of the radiologic findings for histologic types among malignant lesions have been nonspecific and are not well characterized.[10] Dual-phase computed tomography (CT) is considered a useful and reliable tool in preoperative diagnosis and differentiation between benign and malignant lesions of the salivary glands.[11−13] The purpose of this study was to investigate whether there are typical imaging features for SDC on contrast-enhanced CT (CECT) and whether it is possible to differentiate among salivary gland malignancies to narrow the differential diagnosis and assist clinicians in planning treatment.

MATERIALS AND METHODS

Patients

All procedures followed were in accordance with the ethical standards of the responsible committee on human experimentation (institutional and national) and with the Helsinki Declaration of 1975, as revised in 2008 (5). The institutional review board approved this study and waived the need for informed consent. All patients were histopathologically diagnosed with malignant salivary gland tumors and were treated at our institution from January 2012 to October 2018. The inclusion criteria for patients were as follows: (1) surgical resection at our institution with histopathologic confirmation; (2) primary or recurrent lesions; and (3) multiphase CECT scanning before surgery. Of the 107 patients identified, 44 did not meet the

Statement of Clinical Relevance

Multiphase contrast-enhanced computed tomography shows some imaging features, such as ill-defined borders, infiltration into adjacent tissues, heterogeneous masses with cribriform necrosis, and enhancement patterns, which may be useful in the diagnosis of salivary duct carcinoma and differentiating such lesions from other salivary gland malignancies.

[a]Department of Radiology, the First Affiliated Hospital of Chongqing Medical University, Chongqing, China.
[b]Department of Pathology, Chongqing Traditional Chinese Medicine Hospital, Chongqing, China.
[c]Department of Pathology, College of Basic Medicine, Chongqing Medical University, Chongqing, China.
[d]Key Laboratory of Optoelectronic Technology and Systems of the Ministry of Education, Chongqing University, Chongqing, China.
Received for publication Oct 14, 2018; returned for revision May 15, 2019; accepted for publication May 24, 2019.

2212-4403/$-see front matter
https://doi.org/10.1016/j.oooo.2019.05.011

inclusion criteria and were excluded from the study. We therefore analyzed 63 cases, including 9 patients with SDC, 18 with mucoepidermoid carcinoma (MEC), 25 with adenoid cystic carcinoma (ACC), and 11 with acinic cell carcinoma (AcCC). Information regarding clinical findings was obtained through review of the electronic medical records at our institution, and included sex, age, clinical symptoms, symptom duration, and whether the lesion was primary or recurrent.

CT imaging protocol

All CT examinations were performed on a 64-slice GE Discovery 750 HD CT scanner (GE Healthcare, Milwaukee, WI). The scanning parameters were as follows: detector collimation 0.625 mm, pitch 1.375:1, tube voltage 120 kVp, tube current 80 to 270 mAs, and rotation time 0.5 seconds. Non−contrast-enhanced and contrast-enhanced CT was performed. For the CECT scans, approximately 1 to 1.5 mL/kg of the contrast medium Ultravist 370 (Bayer HealthCare LLC, Leverkusen, Germany) was administered into an antecubital vein at a rate of 3 mL/sec. Scanning was performed with 5-mm section thickness from the skull base to the upper thorax, including the entire parotid gland. All patients underwent dual-phase CECT scanning, which was performed during arterial and venous phases with delays of 30 to 40 and 60 to 70 seconds, respectively. Forty-one patients (5 with SDC, 14 with MEC, 13 with ACC, and 9 with AcCC) underwent delayed-phase scanning at 110 to 120 seconds delay.

Imaging analysis

Each CT scan was evaluated independently by 2 head and neck radiologists, who were unaware of the histopathologic diagnoses. The location, size, mass pattern, enhancement pattern, borders, invasion of adjacent tissues, and lymph node metastasis (LNM) were evaluated. Discrepancies, if any, were resolved by consensus. Tumor location was defined as the specific gland involved and as being within the superficial lobe, deep lobe, or both in the parotid gland. Tumor size was measured at maximal cross-sectional dimension. Mass pattern was classified as "solid mass," "cystic mass," or "cystic mass with a mural nodule." The enhancement pattern in the lesions in each phase was categorized as "heterogeneous" or "homogeneous." The borders of the tumors were classified as "ill defined" or "well defined." Every conspicuous invasion into adjacent tissue representing extranodal extension (ENE) was observed. The ENE criteria included central necrosis and irregular nodal enhancement, loss of adjacent fat or muscle planes, and indistinct nodal margins.[14,15] Perineural invasion (PNI) and LNM were examined for each patient.

CT attenuation of the solid part of the tumor at the central level was measured. The ratio of venous-phase CT numbers to arterial-phase CT numbers was calculated. Discrepancies in the categorical parameters, if any, were resolved by consensus. The parameters with quantitative data (size of the lesion and CT number ratios) were analyzed by using the average values entered by the 2 radiologists.

Histopathologic analysis

All pathologic sections of tumors were analyzed retrospectively by 2 pathologists with clinical experience of 8 and 26 years. The sections were stained with hematoxylin and eosin (H&E). Each lesion was diagnosed on the basis of the histomorphologic pattern and cytologic features. The malignancy of the tumor was graded, including SDC; low-, intermediate- and high-grade MEC; solid type ACC (>30% solid component); and low- and high-grade AcCC. Lesions were examined for cystic and/or necrotic patterns. *Extraparenchymal infiltration* was defined as carcinoma invading beyond the capsule. The term *comedonecrosis* was applied when significant necrosis, creating an appearance similar to comedos seen in cutaneous acne, was noted in ducts involved with SDC. PNI involved cancer cells surrounding the nerve fibers and entering the perineurium, resulting in local infiltration and metastasis. The histologic criterion for ENE was defined as the spread of tumor cells beyond the capsule of a metastatic lymph node into the perinodal tissues. The pathologists reached a consensus through discussion if there was a discrepancy in the interpretation of these pathologic results.

Statistical analysis

Statistical analysis was performed by using SPSS software version 17.0 (SPSS Inc., Chicago, IL). The Student *t* test was used to calculate the significance of differences in the mean age of patients, lesion size, CT attenuation (in Hounsfield units), and the ratio of venous-phase CT number to arterial-phase CT number among malignant tumors. Median symptom duration was compared by using the Mann-Whitney U test. Categorical data were compared by using the χ^2 test or Fisher's exact test, as appropriate. A P value less than .05 was considered to indicate a statistically significant difference.

RESULTS

General information and image interpretations of the malignant salivary gland tumors in the 63 study patients are summarized in Table I. Representative illustrations of the lesions are presented for SDC (Figures 1A to 1D), MEC (Figures 1E to 1H), ACC (Figures 1I to 1L), and AcCC (Figures 1M to 1P). The characteristics of the 9 patients with SDC are presented in Table II. There were significant differences in sex between the patients with SDC and those with the other 3 tumor types ($P = .018$).

Table I. Patients' general information and image interpretation of the salivary gland malignancies

Characteristics	*SDC (n = 9)*	*MEC (n = 18)*	*ACC(n = 25)*	*AcCC (n = 11)*	*P value*
Sex					**.018***
Male	9 (100%)	9 (50%)	14 (56%)	4 (36.4%)	
Female	0	9 (50%)	11 (44%)	7 (63.6%)	
Mean age (range)	59.7 ± 6.8 (51−72)*	49.1 ± 17.8 (21−77)	53.4 ± 12.4 (29−73)	44.2 ± 14.8 (22−69)*	–
Median symptom duration	1 year	3 months	1 year	5 years	>.05
Location					**.002***
Parotid gland	6 (66.7%)	16 (88.9%)	10 (40%)	11 (100%)	
Submandibular gland	3 (33.3%)	2 (11.1%)	10 (40%)	0	
Sublingual gland	0	0	5 (20%)	0	
Size (cm): Average	2.66 ± 1.24	2.35 ± 0.88	2.45 ± 0.90	2.41 ± 0.88	>.05
Mass pattern					.143*
Solid mass	8 (88.9%)	15 (83.3%)	24 (96%)	10 (90.9%)	
Cystic mass	0	0	1 (4%)	1 (9.1%)	
Cystic mass with mural nodule	1 (11.1%)	3 (16.8%)	0	0	
Enhancement pattern					.217
Heterogeneous	8 (88.9%)	10 (55.7%)	20 (80%)	7 (63.6%)	
Homogeneous	1 (11.1%)	8 (44.3%)	5 (20%)	4 (36.4%)	
Border					.416
Ill-defined	8 (88.9%)	10 (55.6%)	16 (64%)	7 (63.6%)	
Well-defined	1 (11.1%)	8 (44.4%)	9 (36%)	4 (36.4%)	
Invasion into adjacent tissues	8 (88.9%)	1(5.6%)	5(20%)	1(9.1%)	<**.001***
Perineural invasion	0	0	0	0	>.05
Lymph node metastasis	4 (44.4%)	1 (5.6%)	4 (16%)	0	**.032**

*There were significant differences in sex between the patients with SDC and those with the other 3 tumor types *(P = .018)*. There was statistically significant difference in mean age between SDC and *AcCC (P = .008)*. There were no significant differences in median symptom duration, in the average sizes, in mass pattern *(P = 0.143)* and in border definition *(P = .416)* among the tumor types. Significant differences in location were observed among the different types of malignancies *(P = .002)*. Differences in enhancement patterns among the tumor types were not significant *(P = .217)*. However, invasion into adjacent tissue was significantly more common with *SDC (n = 8 [88.9%])* compared with the other malignancies *(P < .001)*.

ACC, adenoid cystic carcinoma; *AcCC*, acinic cell carcinoma; *MEC*, mucoepidermoid carcinoma; *SDC*, salivary duct carcinoma.

The *P* values for comparisons of SDC with MEC, ACC, and AcCC were 0.012, 0.017, and 0.005, respectively. Patients with SDC were all males, whereas 44% to 63.6% of patients with MEC, ACC, and AcCC were females. SDC patients were significantly older than patients with AcCC (*P* = .008). All patients with SDC presented with movable or fixed masses that were painless (8 [88.9%]) or painful (1 [11.1%]) and of several months' to several years' duration, as indicated in Table II. However, there were no significant differences in median symptom duration among the tumor types. Three patients with SDC (33.3%) complained of facial nerve palsy (weakness or paralysis), as shown in Table II. However, only 1 patient with MEC (5.6%), 5 with ACC (2.0%), and 1 with AcCC (9.1%) were found to have facial nerve palsy.

Significant differences in location were observed among the different types of malignancies (*P* = .002). Two-thirds of SDCs originated in the parotid gland (n = 6 [66.7%]); of these, 5 lesions were located in the deep lobes, and 1 invaded the superficial and deep lobes. The other 3 SDC tumors occurred in the submandibular gland (n = 3 [33.3%]). The majority of MECs (n = 16 [88.9%]) and AcCCs (n = 11 [100%]) arose in the parotid gland, mostly in the superficial lobes. The average size at maximal cross-sectional area was 2.0 × 2.1 cm (range 1.7−5.6 cm). There was no significant difference in the average sizes between the 4 types of tumors. Most SDCs (n = 8 [88.9%]) exhibited a solid mass pattern, isodense with muscle. One lesion was a cystic mass with a nodule, resulting in hypodense attenuation. The differences in mass pattern among the types of malignant lesions were not significant (*P* = 0.143). On CECT images, 8 SDC lesions (88.9%) showed heterogeneous enhancement, and 3 of them presented cribriform necrosis (see Figures 1A to 1D). However, other types of malignancies with necrosis presented with low attenuation centrally (see Figures 1E to 1L). Differences in enhancement patterns among the tumor types were not significant (*P* = .217).

Ill-defined borders were more frequent in SDC (n = 8 [88.9%]) compared with the other tumor types. Many low-grade and intermediate-grade MECs (n = 8 [66.7%]) and low-grade AcCC (n = 4 [57.1%]) exhibited well-defined borders with ring enhancement (see Figures 1M to 1P). Overall, however, there were no significant

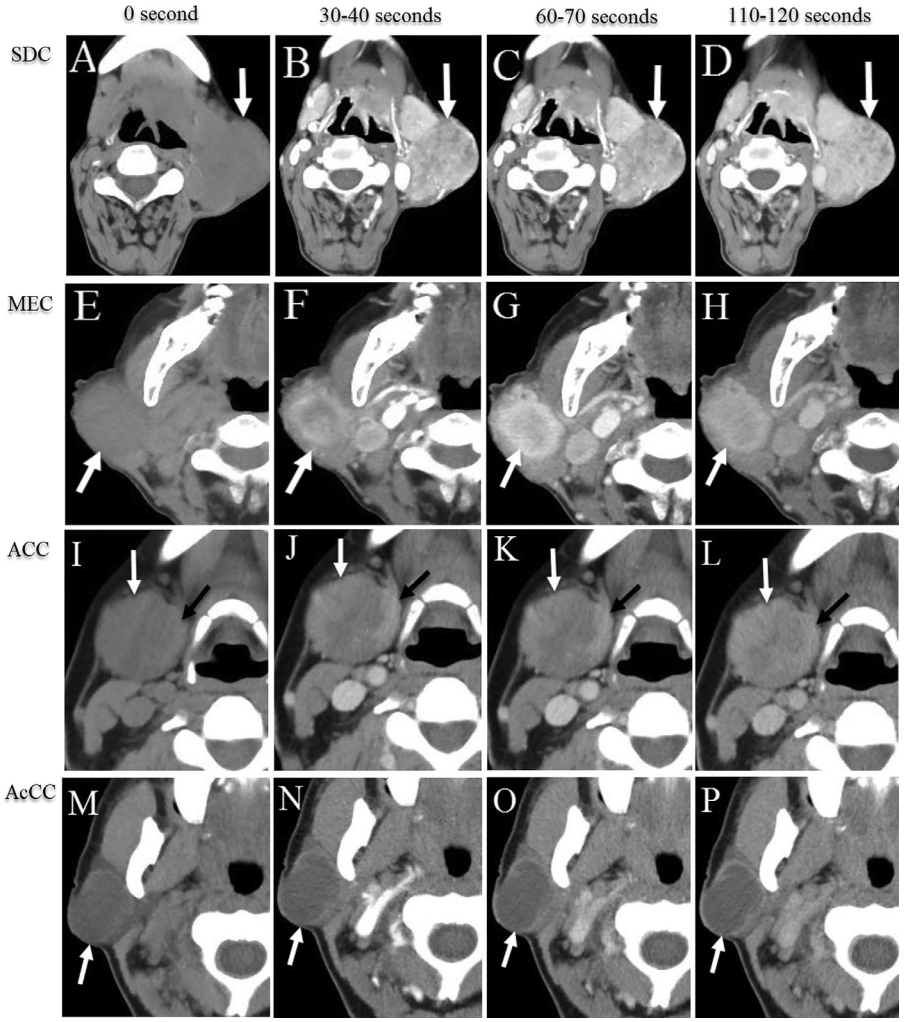

Fig. 1. A−D, Salivary duct carcinoma of the left parotid gland in a 62-year-old man. Contrast-enhanced computed tomography (CECT) images show a large, ill-defined, heterogeneous enhancement of a solid mass involving both superficial and deep lobes of the left parotid gland. The left internal jugular vein is involved directly by the tumor *(not shown)*. The enhancement pattern presents a strongly gradual upward enhancement with cribriform necrosis *(arrows)*. E−H, Mucoepidermoid carcinoma of the right parotid gland in a 77-year-old woman. CECT images show an ill-defined, heterogeneous enhancement of a solid mass *(arrow)* with central low attenuation suggestive of necrosis. The delayed phase image demonstrates decreased enhancement of the tumor *(arrow)*. I−L, Adenoid cystic carcinoma in the right submandibular gland in a 45-year-old woman. CECT images show a large, well-defined soft tissue mass *(white arrows)*. Most of the lesion has a slightly increased attenuation compared with the strongly enhanced mural nodule *(black arrows)*. There is slightly heterogeneous low attenuation in the center of the lesion on postcontrast images. M−P, Acinic cell carcinoma in the right parotid gland in a 55-year-old woman. CECT images reveal a well-defined lesion with ring enhancement *(arrows)* in the superficial lobe of the right parotid gland. There is homogeneously low attenuation in the center of the mass without enhancement.

differences in border definition among the tumor types (P = .416). However, invasion into adjacent tissue was significantly more common with SDC (n = 8 [88.9%]) compared with the other malignancies (P < .001). Tumors invaded the adjacent fat in 3 patients, the skin in 2 patients, and the adjacent sternocleidomastoid, digastric, and masseter muscles in 2 patients (Figures 2A to 2C), which were confirmed intraoperatively or pathologically. Infiltration into the internal jugular vein was detected in 1 SDC. In contrast, only 1 MEC (5.6%), 4 ACCs (16%) and 1 AcCC (9.1%) infiltrated into the adjacent muscles, and 1 ACC invaded the peritumoral fat. ENE was detected in 3 cases of SDC. PNI was not detected radiographically in any patients.

LNM was significantly different among the 4 types of neoplasms (P = .032). Four (44.4%) SDCs metastasized to the cervical lymph nodes, and 3 of them showed ENE. The 3 ENEs had central necrosis with irregular heterogeneous enhancement on CECT, and 2 of them showed loss of the adjacent fat and muscle planes, respectively, producing indistinct nodal margins (Figure 2D).

Table II. The characteristics of nine salivary duct carcinomas

Case/Gender/Age	*Location*	*Clinical symptoms*	*Symptom duration*	*Primary/Recurrence*	*Pathology*				
					Cystic/necrotic	*EPI*	*Comedonecrosis*	*PNI*	*ENE*
1/M/62 years	LPG	Movable painless mass	1 year	Primary	−/+	+	+	+	+
2/M/67 years	LPG	Movable painless mass	1 year	Primary	−/+	+	+	-	-
3/M/60 years	LSMG	Movable painful mass	5 months	Primary	+/−	+	+	-	-
4/M/72 years	LSMG	Movable painless mass; FNP	1 year	Primary	−/+	+	+	+	-
5/M/51 years	RPG	Movable painless mass; FNP	1 year	Primary	−/+	+	−	+	+
6/M/60 years	RPG	Fixed painless mass FNP	15 months	Primary	−/+	+	−	+	+
7/M/52 years	LPG	Fixed painless mass	1 year	Primary	−/+	+	+	-	-
8/M/67 years	RSMG	Movable painless mass	6 months	Recurrence	−/+	+	+	-	+
9/M/56 years	LPG	Movable painless mass	6 months	Recurrence	−/−	+	−	+	-

ENE, extranodal extension; EPI, extraparenchymal infiltration; FNP, facial nerve palsy; LPG, left parotid gland; LSMG, left submandibular gland; PNI, perineural invasion; RPG, right parotid gland; RSMG, right submandibular gland.

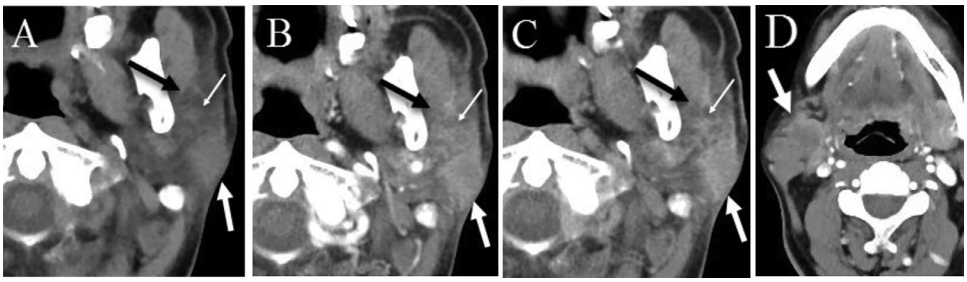

Fig. 2. **A**−**C,** Salivary duct carcinoma of the left parotid gland in a 67-year-old man. Contrast-enhanced computed tomography (CECT) images show an ill-defined mass *(white thick arrows)* with homogeneous enhancement. The left masseter muscle *(black arrows)*, normal parotid tissue, and peritumoral fat *(white thin arrows)* are invaded by the tumor. **D,** Salivary duct carcinoma with lymph node metastases in a 67-year-old man. An arterial phase image shows a metastatic enlarged right level IIA lymph node *(arrow)* with ill-defined borders and loss of the adjacent fat plane. There is heterogeneous enhancement of the node with central low attenuation suggestive of necrosis.

The CT numbers for different types of malignant tumors of the salivary glands are listed in Table III. As shown in Table III and Figure 3, each histopathologic type of tumor presented early enhancement during arterial-phase scanning, with increased attenuation during the venous phase. SDCs presented slightly increased attenuation during delayed-phase scanning, whereas other types of malignant tumors showed decreased attenuation. However, only 1 of 5 SDCs showed increased attenuation during delayed-phase scanning.

SDC exhibited a significantly higher mean CT number compared with ACC during delayed-phase scanning ($P = .031$). ACC had a lower CT number during arterial-phase scanning compared with the other types of malignant tumors, including a significant difference with MEC ($P = .047$). In addition, ACC also had a

Table III. The mean ± SD CT numbers of salivary gland malignancies on multiphase CECT

Histopathologic subtypes	*CT No. in plain scanning (HU)*	*CT No. in arterial-phase scanning (HU)*	*CT No. in venous-phase scanning (HU)*	*CT No. in delayed-phase scanning (HU)**	*Ratio of CT No.*
SDC (n = 9)	50.11 ± 8.33	93.00 ± 16.01	105.00 ± 16.40	108.80 ± 17.38†	1.15 ± 0.22
MEC (n = 18)	47.28 ± 10.21	99.17 ± 28.43‡	102.50 ± 21.04	101.00 ± 20.41	1.06 ± 0.22§
ACC (n = 25)	43.96 ± 11.43	78.54 ± 34.77‡	92.88 ± 20.99	85.31 ± 19.33†	1.27 ± 0.32§
AcCC (n = 11)	51.10 ± 11.56	87.70 ± 22.54	92.00 ± 15.65	86.67 ± 19.79	1.07 ± 0.16

*Only 41 of the 63 patients (5 with SDCs, 14 with MECs, 13 with ACCs, and 9 with AcCC) underwent delayed-phase scanning at 110- to 120-second delay.

†SDC had significantly higher mean CT numbers during delayed-phase scanning compared with ACC ($P = .031$).

‡ACC had significantly lower mean CT number during arterial-phase scanning compared with MEC ($P = .047$).

§ACC had a significantly higher ratio of CT numbers compared with MEC ($P = .018$).*ACC,* adenoid cystic carcinoma; *AcCC,* acinic cell carcinoma; *CT,* computed tomography; *HU,* Hounsfield unit; *MEC,* mucoepidermoid carcinoma; *No.,* number; *SDC,* salivary duct carcinoma.

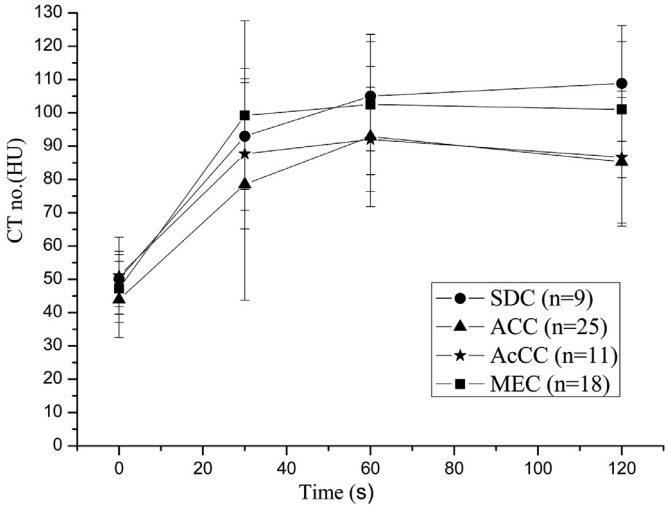

Fig. 3. Time attenuation curves for salivary duct carcinoma (SDC), mucoepidermoid carcinoma (MEC), adenoid cystic carcinoma (ACC), and acinic cell carcinoma (AcCC). All types of tumors present early enhancement. SDC shows slightly increased attenuation during delayed-phase scanning, whereas the other types of malignancies show a decrease in attenuation. Error bars indicate standard deviations (SDs).

significantly higher ratio of CT numbers compared with MEC ($P = .018$). However, there were no significant differences in the mean attenuation among all of the histopathologic tumor types during plain scanning or during venous-phase scanning ($P > .05$).

Histopathologic results

There were 9 SDCs, 12 low- and intermediate-grade MECs, 6 high-grade MECs, 4 solid type ACCs, 7 low-grade AcCCs, and 4 high-grade AcCCs. SDC had a striking resemblance to high-grade ductal carcinoma of the breast, including intraductal and infiltrating components. SDC cells are typically apocrine or oncocytoid and characterized by abundant cytoplasm and large pleomorphic nuclei with coarse chromatin and prominent nucleoli. Only 1 lesion was cystic, but 7 of 9 tumors exhibited necrosis. All SDCs had incomplete capsules and invasive borders showing extraparenchymal infiltration. In the infiltrated zones, tumor cells, fibrosis, and necrosis were mixed at various proportions. Six tumors (66.7%) had comedonecrosis in the center of the duct. Neoplastic cells invaded the peritumoral fat in 6 SDCs. PNI was observed in 5 SDC patients (55.6%). Four (44.4%) of the 9 SDCs had metastatic lymph nodes, and all of them showed ENE.

DISCUSSION

It has been reported that SDC predominantly arises from the parotid gland, shows a male predilection, and generally affects older individuals. The most common symptom is a rapidly enlarging, painless or painful mass with facial paralysis. These observations are in agreement with the present findings.[5,16–18]

Previous studies have described imaging features of salivary gland tumors.[7,8,10] However, the appearance of malignant tumors is not specific for pathologic types.[7,10,19] This is especially true with non−CECT, in which many malignancies have a heterogeneous mass, ill-defined borders, and invasion into adjacent tissues. We used multiphase CECT in an attempt to differentiate various salivary gland malignant tumors before surgery. The CECT findings in this study reflect the pathologic features of SDC. The tumor was characterized as having both intraductal and infiltrating components on histopathologic examination. Comedonecrosis was the most common finding for the intraductal component. The enhancement pattern was heterogeneous enhancement with cribriform necrosis, which may be a special feature of SDC and, therefore, useful in formulating a differential diagnosis. The infiltrating component is occasionally accompanied by abundant fibrotic stroma.[20] The present study yielded similar results. This pathologic feature seemed to reflect the gradual upward enhancement pattern, which can explain why SDC presented slightly increased attenuation, whereas the other types of malignant tumors showed decreased attenuation during delayed-phase scanning. Motoori et al.[19] also reported that SDC frequently has a gradual upward enhancement that may be associated with prominent fibrosis. However, our data showed that most SDCs also presented decreased attenuation during delayed-phase scanning, which is consistent with the enhancement pattern of malignant tumors.[11–13,19] According to Tsushima et al.[21] malignant parotid tumors, except for MEC, ACC, and AcCC, show early enhancement. Our data also revealed that ACC had a lower CT number during arterial-phase scanning compared with the other types of malignant tumors, and there was a statistically significant difference between MEC and ACC ($P = .047$). The ratio of CT numbers was significantly

different between MEC and ACC ($P = .018$). Based on these findings, multiphase CECT could provide some features of SDC and CT numbers at different phases, and this would be useful in the differential diagnosis of malignant salivary gland tumors, especially for discriminating ACC from SDC and MEC.

Pathologically, the tumors tended to be noncapsulated with invasive growth patterns, reflected by ill-defined borders and visible infiltration on CECT images. Junn et al.[22] investigated muscle invasion on radiologic evaluation and found that CECT is sensitive (100%) for muscle invasion but has reduced specificity (76%) compared with intraoperative surgical and pathologic consensus evaluation. Therefore, those authors concluded that intraoperative surgical and pathologic evaluation should be encouraged to verify radiologic muscle invasion. In the present study, the overlying peritumoral fat, skin, adjacent muscles, and vessels were invaded by SDCs, and this was confirmed intraoperatively or pathologically and was more common in SDCs than in the other types of salivary malignancies ($P < .001$). These invasions indicate stage T4 in salivary tumors, suggesting that preoperative CT plays an important role in tumor (T) staging, clinical treatment decisions, and patient prognosis.

In this study, 5 patients with SDC (55.6%) presented with PNI on histologic examination, and in 3 of them, the findings were in accordance with their clinical symptoms, such as facial nerve palsy. These observations are in agreement with 28% to 85% of patients with SDC and PNI.[23] The superficial and deep lobes of the parotid gland are separated by the facial nerve, which gives rise to the 5 terminal branches within the gland, which then innervate the muscles of facial expression. According to our results, SDC predominantly arose from the parotid gland, which can explain why facial nerve palsy was more common in SDC. Small branches of PNI cannot easily be detected on CT. However, CT can be sensitive with regard to widening or erosion of skull base foramina or canals and obliteration of the normal fat density within the foramina or within the pterygopalatine fossa.[24] There was no CECT evidence of PNI in the 9 SDCs in this study. Magnetic resonance imaging (MRI), especially contrast-enhanced, fat-suppressed, small field-of-view sequences, is advantageous for evaluating nerve invasion.[24] In our study, MRI images of SDC were not available, and this was the major limitation of this study.

SDC has a propensity to metastasize early to regional lymph nodes (approximately 20%−71%) and distant sites and has a rate of local recurrence of approximately 13% to 48%.[2,5,23,25] In this study, the frequency of LNM in SDC was higher compared with that in the other types of salivary gland malignancies ($P = .032$). We diagnosed 4 patients with ENE confirmed by pathology, whereas only 3 were considered ENE on CECT. The presence of extracapsular spread in metastatic cervical lymph nodes portends poor distant control and prognosis for head and neck tumors.[15,26] ENE can be visualized with the use of multiple imaging modalities, and this helps determine tumor staging and treatment planning and predict the prognosis. In some studies, necrosis on imaging has the highest accuracy in classification, and irregular borders and gross invasion have been independently correlated with pathologically proven extracapsular spread.[14,15] However, the specificity of cross-sectional imaging for ENE is high, and the sensitivity is low.[14,15] In this study, centrally necrotic nodes showed heterogeneous enhancement on CECT, which was well correlated with pathologic ENE. Approximately 32% to 62% of SDC exhibit distant metastasis.[3] In general, ^{18}F-fluoro-2-deoxyglucose−positron emission tomography (PET) is considered complementary and sometimes superior to anatomic imaging modalities for staging and restaging of salivary gland malignancies.[27] The use of PET/CT usually shows SDC as a highly metabolic tumor and can be quite useful for detecting regional and distant metastases.[28] If SDC is suspected, especially in patients with extensive nodal disease, PET/CT should be performed to rule out distant metastasis.

Differential diagnosis

MEC is the most common malignant tumor of the salivary glands. The imaging features of the tumor in this investigation depended on the histologic type. Low-grade and intermediate-grade MECs had well-defined borders with a round form, which helped easily differentiate them from SDCs. In contrast, high-grade lesions tended to appear more ill-defined and aggressive. However, invasion into adjacent tissues was significantly less common in MEC than in SDC.

ACC, the second most common malignant salivary gland tumor, originates from the parotid, submandibular, and sublingual glands, as seen in the present study. There was a significant sex difference between SDC and ACC ($P = .017$). ACC presented heterogeneous enhancement and ill-defined borders and sometimes exhibited LNM. These findings are consistent with those reported previously.[29,30] The CT numbers of SDC and ACC during delayed-phase scanning may be useful in differentiating them because we observed that SDC has significantly greater attenuation compared with ACC ($P = .031$).

AcCC is a rare epithelial salivary gland tumor with a longer growth duration. The mean age was approximately 44.2 years, which was significantly less than that of patients with SDC ($P = .008$). In addition, AcCC had a relatively equal sex distribution, with a slight female predilection, whereas SDC had a clear male predilection ($P = .005$). Sex and age, therefore, may be helpful in formulating a differential diagnosis. The imaging characteristics of AcCC were nonspecific and can present benign

or malignant features. These findings are consistent with those reported previously.[31,32] Metastases to regional lymph nodes has been reported in 10% to 19% of patients,[31,32] lower than the percentage of patients with SDC and LNM. Our results confirm this finding, with no AcCC exhibiting LNM.

Parotid tumors are the most frequent salivary gland tumors, and approximately 20% to 25% are malignant.[33] In this study, high-grade parotid gland tumors included 9 SDCs, 6 high-grade MECs, 4 solid type ACCs, and 4 high-grade AcCCs. Clinically, they presented as painful, movable masses. However, facial nerve palsy and LNM were more common in SDC than in the other types of parotid gland malignancies. With respect to sex distribution, AcCC had a slight female predilection, whereas SDC and ACC had a male predilection. Most SDCs were located in the deep lobes, whereas most parotid high-grade MECs and AcCCs were found in the superficial lobes. Heterogeneous enhancement, ill-defined borders, and invasion into adjacent tissues can be seen in all types of malignant tumors. However, the frequency of invasion of SDC was significantly greater than in the other neoplasms. SDC should be strongly considered when the patient is an older male with a mass in the deep lobe of the parotid gland that exhibits heterogeneous enhancement with a cribriform necrosis pattern, invasion into adjacent tissues, and LNM on CECT.

CONCLUSIONS

SDC is a rare, high-grade malignant tumor of the salivary gland, characterized clinically by predilection for older males and facial paralysis combined with a rapidly enlarging, painless or painful mass. The tumor predominantly arises in the parotid gland, especially in the deep lobe. The imaging findings on non−CECT are nonspecific. CECT features often include a solid mass pattern; heterogeneous enhancement, sometimes with cribriform necrosis; ill-defined borders; infiltration into adjacent tissues; and LNM with extranodal extension. The lesion is associated with comedonecrosis and ENE on histopathologic evaluation. These features may be useful in formulating a diagnosis of SDC. Multiphase CECT imaging with an enhancement pattern may be a useful method in establishing differential diagnoses in salivary gland tumors, especially for distinguishing SDC from MEC and ACC.

SUPPLEMENTARY MATERIALS

Supplementary material associated with this article can be found in the online version at doi:10.1016/j.oooo.2019.05.011.

REFERENCES

1. El-Naggar AK, JKC C, Grandis JR, Takata T, Slootweg PJ. Tumours of salivary glands. In: WHO Classification of Head and Neck Tumours. Lyon, France: IARC Press; 2017. p. 159-202.
2. Seethala RR, Stenman G. Update from the 4th edition of the World Health Organization Classification of Head and Neck Tumours: Tumors of the Salivary Gland. *Head Neck Pathol*. 2017;11:55-67.
3. Gilbert MR, Sharma A, Schmitt NC, et al. A 20-Year review of 75 cases of salivary duct carcinoma. *JAMA Otolaryngol Head Neck Surg*. 2016;142:489-495.
4. Johnston ML, Huang SH, Waldron JN, et al. Salivary duct carcinoma: treatment, outcomes, and patterns of failure. *Head Neck*. 2016;38:E820-E826.
5. Jang JY, Choi N, Ko YH, et al. Treatment outcomes in metastatic and localized high-grade salivary gland cancer: high chance of cure with surgery and post-operative radiation in T1−2 N0 high-grade salivary gland cancer. *BMC Cancer*. 2018;18:672.
6. You HJ, Yun TK, Jeong SH, Dhong ES, Han SK. Salivary duct carcinoma of the deep lobe of the parotid gland: a rare clinical finding. *Arch Plast Surg*. 2016;43:107-110.
7. Weon YC, Park SW, Kim HJ, et al. Salivary duct carcinomas: clinical and CT and MR imaging features in 20 patients. *Neuroradiology*. 2012;54:631-640.
8. Habermann CR, Arndt C, Graessner J, et al. Diffusion-weighted echo-planar MR imaging of primary parotid gland tumors: is a prediction of different histologic subtypes possible? *AJNR Am J Neuroradiol*. 2009;30:591-596.
9. Huh KH, Heo MS, Lee SS, Choi SC. Three new cases of salivary duct carcinoma in the palate: a radiologic investigation and review of the literature. *Oral Surg Oral Med Oral Pathol Oral Radiol Endod*. 2003;95:752-760.
10. Gamoh S, Akiyama H, Tsuji K, et al. Non-contrast computed tomography and magnetic resonance imaging features of mucoepidermoid carcinoma in the salivary glands. *Oral Radiol*. 2018;34:24-30.
11. Choi DS, Na DG, Byun HS, et al. Salivary gland tumors: evaluation with two-phase helical CT. *Radiology*. 2000;214:231-236.
12. Joo YH, Kim JP, Park JJ, Woo SH. Two-phase helical computed tomography study of salivary gland Warthin tumors: a radiologic findings and surgical applications. *Clin Exp Otorhinolaryngol*. 2014;7:216-221.
13. Woo SH, Choi DS, Kim JP, et al. Two-phase computed tomography study of warthin tumor of parotid gland: differentiation from other parotid gland tumors and its pathologic explanation. *J Comput Assist Tomogr*. 2013;37:518-524.
14. Aiken AH, Poliashenko S, Beitler JJ, et al. Accuracy of preoperative imaging in detecting nodal extracapsular spread in oral cavity squamous cell carcinoma. *AJNR Am J Neuroradiol*. 2015;36:1776-1781.
15. Carlton JA, Maxwell AW, Bauer LB, et al. Computed tomography detection of extracapsular spread of squamous cell carcinoma of the head and neck in metastatic cervical lymph nodes. *Neuroradiol J*. 2017;30:222-229.
16. Jayaprakash V, Merzianu M, Warren GW, et al. Survival rates and prognostic factors for infiltrating salivary duct carcinoma: analysis of 228 cases from the Surveillance, Epidemiology, and End Results database. *Head Neck*. 2014;36:694-701.
17. D'heygere E, Meulemans J, Vander Poorten V. Salivary duct carcinoma. *Curr Opin Otolaryngol Head Neck Surg*. 2018;26:142-151.
18. Jaehne M, Roeser K, Jaekel T, Schepers JD, Albert N, Löning T. Clinical and immunohistologic typing of salivary duct carcinoma: a report of 50 cases. *Cancer*. 2005;103:2526-2533.
19. Motoori K, Iida Y, Nagai Y, et al. MR imaging of salivary duct carcinoma. *AJNR Am J Neuroradiol*. 2005;26:1201-1206.
20. Hosal AS, Fan C, Barnes L, Myers EN. Salivary duct carcinoma. *Otolaryngol Head Neck Surg*. 2003;129:720-725.
21. Tsushima Y, Matsumoto M, Endo K. Parotid and parapharyngeal tumours: tissue characterization with Dynamic magnetic resonance imaging. *Br J Radiol*. 1994;67:342-345.

22. Junn JC, Baugnon KL, Lacayo EA, et al. CT accuracy of extrinsic tongue muscle invasion in oral cavity cancer. *AJNR Am J Neuroradiol*. 2017;38:364-370.
23. Huang X, Hao J, Chen S, Deng R. Salivary duct carcinoma: a clinopathological report of 11 cases. *Oncol Lett*. 2015;10:337-341.
24. Seeburg DP, Baer AH, Aygun N. Imaging of patients with head and neck cancer: from staging to surveillance. *Oral Maxillofac Surg Clin North Am*. 2018;30:421-433.
25. Johnston ML, Huang SH, Waldron JN, et al. Salivary duct carcinoma: treatment, outcomes, and patterns of failure. *Head Neck*. 2016;38:E820-E826.
26. Kann BH, Buckstein M, Carpenter TJ, et al. Radiographic extracapsular extension and treatment outcomes in locally advanced oropharyngeal carcinoma. *Head Neck*. 2014; 36:1689-1694.
27. Bertagna F, Nicolai P, Maroldi R, et al. Diagnostic role of (18)F-FDG-PET or PET/CT in salivary gland tumors: a systematic review. *Rev Esp Med Nucl Imagen Mol*. 2015; 34:295-302.
28. Kim JY, Lee SW, Kim JS, et al. Diagnostic value of neck node status using 18 F-FDG PET for salivary duct carcinoma of the major salivary glands. *J Nucl Med*. 2012;53:881-886.
29. Uraizee I, Cipriani NA, Ginat DT. Adenoid cystic carcinoma of the oral cavity: radiology-pathology correlation. *Head Neck Pathol*. 2018;12:562-566.
30. Netto Jde N, Miranda AM, da Silveira HM, dos Santos TC, Pires FR. Fine needle aspiration biopsy as an auxiliary diagnostic tool on intraoral minor salivary gland adenoid cystic carcinoma. *Oral Surg Oral Med Oral Pathol Oral Radiol Endod*. 2008;106:242-245.
31. Suh SI, Seol HY, Kim TK, et al. Acinic cell carcinoma of the head and neck: radiologic-pathologic correlation. *J Comput Assist Tomogr*. 2005;29:121-126.
32. Sakai O, Nakashima N, Takata Y, Furuse M. Acinic cell carcinoma of the parotid gland: CT and MRI. *Neuroradiology*. 1996;38:675-679.
33. Bradley PJ, McGurk M. Incidence of salivary gland neoplasms in a defined UK population. *Br J Oral Maxillofac Surg*. 2013; 51:399-403.

Reprint requests:

Sheng-sheng Xu
1 Youyi Rd
Chongqing 400016
People's Republic of China
2792917719@qq.com